

# Resonant activation driven by strongly non-Gaussian noises.

Bartłomiej Dybiec\* and Ewa Gudowska-Nowak†

Marian Smoluchowski Institute of Physics,  
Jagellonian University, Reymonta 4,  
30-059 Kraków, Poland

(Dated: July 3, 2018)

The constructive role of non-Gaussian random fluctuations is studied in the context of the passage over the dichotomously switching potential barrier. Our attention focuses on the interplay of the effects of independent sources of fluctuations: an additive stable noise representing non-equilibrium external random force acting on the system and a fluctuating barrier. In particular, the influence of the structure of stable noises on the mean escape time and on the phenomenon of resonant activation (RA) is investigated. By use of the numerical Monte Carlo method it is documented that the suitable choice of the barrier switching rate and random external fields may produce resonant phenomenon leading to the enhancement of the kinetics and the shortest, most efficient reaction time.

PACS numbers: 02.50.-r, 05.10.-a, 05.90.+m, 82.20.-w

## I. INTRODUCTION

The fluctuating barrier problem seems to be of relevance especially for the kinetics of biophysical systems [1, 2, 3, 4] whose time-evolution is governed by coupling to protein molecules undergoing constant conformational transitions. In particular, it is by now well established that membrane proteins that conduct many chemical and physical processes can exist in several conformational states whose distinct electrical properties may be responsible for the efficiency of ionic transport through biological channels. In such cases, the assumption of random fluctuations in the membrane potential has been shown [2, 5] to be sufficient to explain experimental data on active ionic flow and resonance between internal fluctuations and external driving AC field. The enhancement or optimisation of the action of the external regular field by stochastic fluctuations gained the term *stochastic resonance* (SR) and became an issue of vivid experimental and theoretical studies [6] over the past 20 years. Although the SR phenomenon is commonly described as a cooperative effect in which small periodic influence entrains external random noise, similar constructive effects of noises under nonequilibrium constraints can be expected in “ratchet” systems [7] where spatially uniform mean-zero symmetrical (random or periodic) time dependent forces interact with an underlying spatial anisotropy to induce motion. Another resonant-type, noise-induced behaviour [1, 8, 9, 10] is resonant activation (RA), the phenomenon in which an optimal fluctuation rate exists which minimizes the mean first passage time for the escape over the fluctuating barrier. The generic theoretical models analysing the aforementioned resonant phenomena are usually based on a Langevin equation ap-

proach assuming the overdamped limit [1, 6, 11, 12]. Accordingly, the influence of the external thermal bath of the surroundings on a Brownian particle is described in such an equation by time-dependent random force which is commonly assumed to be represented by a white Gaussian noise. That postulate is compatible with the assumption of a short correlation time of fluctuations, much shorter than the time-scale of the macroscopic motion and assumes that weak interactions with the bath lead to independent random variations of the parameter describing the motion. In more formal, mathematical terms Gaussianity of the state-variable fluctuations is a consequence of the Central Limit Theorem which states that normalized sum of independent and identically distributed (*i.i.d*) random variables with finite variance converges to the Gaussian probability distribution. If, however, after random collisions jump lengths are ruled by broad distributions leading to the divergence of the second moment, the statistics of the process changes significantly. The existence of the limiting distribution is then guaranteed by the generalized Lévy-Gnedenko [13] limit theorem. According to the latter, normalized sums of independent, identically distributed random variables with infinite variance converge in distribution to the Lévy statistics. At the level of the Langevin equation, Lévy noises are generalization of the Brownian motion and describe results of strong collisions between the test particle and the surrounding environment. In this sense, they lead to different models of the bath that go beyond a standard “close-to-equilibrium” Gaussian description [14, 15, 16, 17].

In this communication we present numerical results for the mean first passage time over a fluctuating barrier for the model system with a linear potential subject to Markovian dichotomous fluctuations and additive Lévy noises. We report here on a new phenomenon of reappearance of RA in a model system whose pattern of the most efficient kinetics has been smeared out and destroyed by the presence of driving  $\alpha$ -stable noise. In

\*Electronic address: bartek@th.if.uj.edu.pl

†Electronic address: gudowska@th.if.uj.edu.pl

particular, we demonstrate that a congruent tuning of noise asymmetry with its stability index responsible for scaling properties of the noise increments can optimize the passage over the conformationally changing barrier.

## II. THE MODEL

An overdamped Brownian particle is moving in a potential field between absorbing ( $x = 1$ ) and reflecting ( $x = 0$ ) boundaries, in the presence of noise that modulates the barrier height. Time evolution of a state variable  $x(t)$  is described in terms of the generalized Langevin equation

$$\frac{dx}{dt} = -V'(x) + g\eta(t) + \sqrt{2}\zeta(t) = -V'_{\pm}(x) + \sqrt{2}\zeta(t), \quad (1)$$

where prime means differentiation over  $x$ ,  $\zeta(t)$  is a white Lévy process originating from the contact with non-equilibrated bath and  $\eta(t)$  stands for a Markovian dichotomous noise of intensity  $g$  taking one of two possible values  $\pm 1$ . Autocorrelation of the dichotomous noise is set to  $\langle(\eta(t) - \langle\eta\rangle)(\eta(t') - \langle\eta\rangle)\rangle = \exp(-2\gamma|t - t'|)$ . For simplicity, throughout the paper a particle mass, a friction coefficient and the Boltzman constant are all set to 1. The time-dependent potential  $V_{\pm}(x)$  is assumed to be linear with the barrier switching between two configurations with an average rate  $\gamma$

$$V_{\pm}(x) = H_{\pm}x, \quad g = \frac{H_- - H_+}{2}. \quad (2)$$

Both  $\zeta$  and  $\eta$  noises are assumed to be statistically independent.

The initial condition for Eq. (1) is  $x(0) = 0$ , so that initially particle is located at the reflecting boundary with equal choices of finding a potential barrier in any of two possible configurations ( $\pm$ ). The quantity of interest is the mean first passage time (MFPT), the average time which particle spends in the system before it becomes absorbed. In the approach applied herein information on the MFPT is drawn from the statistics of numerically generated trajectories satisfying the generalized Langevin equation (1) and the examined MFPT is estimated as a first moment of the distribution of first passage times (FPT) obtained from the ensemble of simulated realizations of the stochastic process in question. More precisely, frequency of FPT is calculated as frequency of the time-duration  $\tau$  of the events (trajectories) that have initially started from  $x = 0$  and reached  $x = 1$  for the first time. The MFPT is estimated as  $\langle\tau\rangle$  over the frequency distribution. Despite the fact that in Eq. (1)  $x$  itself is a random variable distributed according to some unknown stable distribution, the FPTs are distributed according to some unknown probability distribution possessing all moments.

## III. RESULTS OF SIMULATIONS

Generally, for systems driven by Gaussian noises, noise-induced phenomena are studied solely in terms of  $\sigma^2$ , the intensity of the white noise [6, 18]. Thermodynamic definition of this noise-source relates  $\sigma^2$  to the system temperature. It is not so, however, for dynamic systems perturbed by Lévy stable noises, for which an appropriate choice of a control parameter is less obvious. It is caused by the fact that stable distributions are characterized by a four-parameter family: the stability index  $\alpha$  ( $\alpha \in (0, 2]$ ), skewness parameter  $\beta$  ( $\beta \in [-1, 1]$ ), the shift  $\mu$  ( $\mu \in \mathbb{R}$ ) and scaling  $\sigma$  ( $\sigma \in \mathbb{R}^+$ ) parameters, respectively (for the definition of Lévy measure, see Appendix A). The PDFs of stable distributions demonstrate asymptotic power-law behaviour according to  $L(\zeta) \approx |\zeta|^{-1-\alpha}$  [13, 19]. The parameter  $\mu$  controls the position of the PDF modal value, whereas  $\sigma$ , similarly to the Gaussian case, scales the width of the distribution. At the first glance, the parameter  $\sigma$  is somehow connected to the system temperature, although the relation is more subtle since stable additive noises can be expected in nonequilibrium situations where the definition of temperature loses its common sense [14, 17].

For the purpose of simulations the value of  $\mu$  has been arbitrary set to 0 and  $\sigma = 1/\sqrt{2}$ . Such a choice of  $\mu$  and  $\sigma$  reconstructs standard normal distribution  $N(0, 1)$  for  $\alpha = 2$ , therefore allowing for comparison of the results obtained in this study with the former ones [1, 11, 12], where the Gaussian measures of the  $\zeta$  noise have been used. Remaining parameters ( $\alpha$  and  $\beta$ ) have taken values from the allowed range with a lower limit set up for the  $\alpha$  value ( $\alpha < .2$  have not been investigated). The RA phenomenon has been examined for various barrier setups: The potential barrier has been switching between different heights  $H_+$  and  $H_-$  and as values of  $H_{\pm}$  the sets  $\pm 8$ ;  $(0, 8)$ ; and  $(4, 8)$  have been chosen. They correspond to the changing of the potential barrier between the barrier and the well ( $H_{\pm} = \pm 8$ ), the barrier and “no barrier” ( $H_+ = 8, H_- = 0$ ) situations and to two barriers with different heights ( $H_+ = 8, H_- = 4$ ).

In order to test the implemented numerical procedures (cf. Appendix A), MC solutions of Eq. (1) for  $\alpha = 2$  have been compared with the exact solutions to the backward Fokker Planck Equation [1, 11]. The numerical results (see Fig. 1) have shown a perfect agreement with the exact solutions.

Subsequent figures demonstrate results of the analysis for driving stable noises with various values of the  $(\alpha, \beta)$  parameters. For the sake of clarity of the comparison, they have been grouped in three classes corresponding to different scenarios of barrier-alteration. The first group (Figs. 2 and 3) relates to the potential barrier switching between  $H_{\pm} = \pm 8$ , Figs. 4 and 5 describe numerical results obtained for the barrier switching between  $H_+ = 8$  and  $H_- = 0$  and, eventually, Figs. 6 and 7 refer to simulations performed for the potential barrier switching between two different barriers, i.e.  $H_+ = 8, H_- = 4$ . In

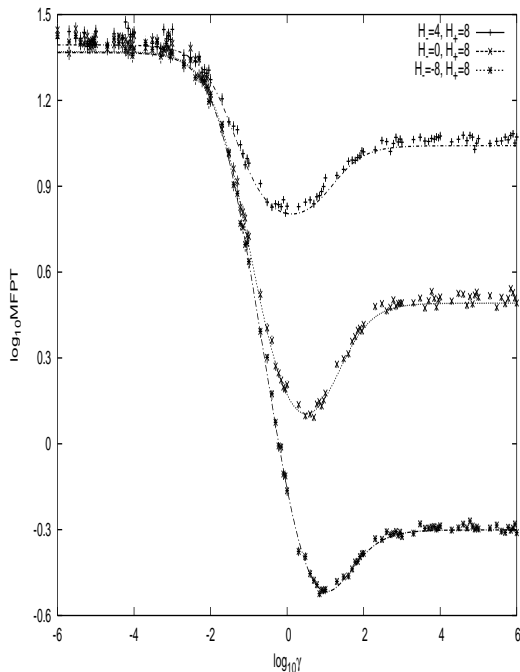


FIG. 1: MFPT( $\gamma$ ) for linear potential barriers switching between different heights  $H_{\pm}$ : (+)  $H_{+} = 8$ ,  $H_{-} = 4$ ; ( $\times$ )  $H_{+} = 8$ ,  $H_{-} = 0$ ; (\*)  $H_{+} = 8$ ,  $H_{-} = -8$ . The driving noise is Lévy stable noise with  $\alpha = 2$ , i.e. Gaussian noise. Solid lines represent exact result constructed by direct integration of the backward Fokker–Planck equation. Numerical results were obtained by use of Monte Carlo simulation of Eq. (1) with time step  $dt = 10^{-4}$  and averaged over  $N = 10^3$  realizations. Error bars represent deviation from the mean and usually remain within the symbol size.

each class, in the first (left) plot (cf. Figs. 2, 4 and 6) the results for fixed  $\beta$  ( $\beta = 0$ ), i.e. for the symmetric stable noises are displayed while the right panel presents results for a fixed value of  $\alpha$  ( $\alpha = 0.5$ ), thus demonstrating the effect of the asymmetry of the driving noise. The second set of plots in each class (cf. Figs. 3, 5 and 7) presents results for the MFPT( $\alpha, \gamma$ ) for a fixed  $\beta$  parameter ( $\beta = 1$ ) while a corresponding right panel displays sample cross-sections of the MFPT( $\alpha, \gamma$ ) surface.

Closer examination of Figs. 2 and 3 allows to conclude that a typical, non-monotonic character of the MFPT curve is preserved for all values of the  $\alpha$  parameter. The only visible changes are registered in the asymptotic behavior and in the depth of the MFPTs curves. In particular, the values of MFPTs for the Gaussian case ( $\alpha = 2$ ) are higher than for other values of  $\alpha$  thus demonstrating that the heavier tails in PDFs (and therefore higher probability of experiencing larger fluctuations) of driving random forces facilitate the transport over the fluctuating barrier. Furthermore, as it can be seen in the right panel of Fig. 2, for  $\alpha = 0.5$  the RA phenomenon is observed for all values  $\beta$ .

In Fig. 3 MFPT( $\alpha, \gamma$ ) surfaces for asymmetric sta-

ble noises ( $\beta = 1$ ) are presented. Interestingly, the MFPT( $\alpha, \gamma$ ) surface for asymmetric ( $\beta = 1$ ) driving noise displays an unexpected behavior. Namely, a gradual change of the  $\alpha$  parameter (from  $\alpha = 0.2$  to  $\alpha = 1.1$ ) results in suppression of the RA phenomenon that disappears for values of  $\alpha \approx 1$  but becomes further recovered for  $\alpha > 1$  approaching  $\alpha$  representative for the Gaussian case. By comparison (cf. Fig. 4, left panel), in the cases when the dynamics flickers between the motion over the erected potential barrier and a free (symmetric) Lévy flight, the characteristic resonant shape of the MFPT curve disappears with a decrease of the stability index  $\alpha$ , i.e. noises with heavier asymptotic tails destroy the RA. Contrary to the  $H_{\pm} = \pm 8$  case, for  $\alpha = 0.5$ , the RA phenomenon is not observed, independently of the value of  $\beta$  (cf. Fig. 4, right panel). However, for asymmetric stable noises (Fig. 5) the same kind of behavior which has been observed for  $H_{\pm} = \pm 8$  can be noticed. Here again, it is possible to detect an optimal  $\alpha$ -value at which activation processes are more efficient (they lead to lower values of the MFPT than for all other choices of the  $\alpha$  parameter). Unlike in the  $H_{\pm} = \pm 8$  case, the RA does not take now place for very small values of  $\alpha$  but it reappears for  $\alpha \approx 1$  when the resonant shape of the MFPT curve becomes clearly visible. Afterwards, for moderate  $\alpha$  the RA phenomenon disappears and, as expected, becomes again induced for  $\alpha = 2$ .

Figs. 6 and 7 display results for  $H_{+} = 8, H_{-} = 4$ . As can be observed in the left panel of Fig. 6, the Gaussian behavior of the MFPT curve disappears with decrease of the stability index  $\alpha$  for symmetric stable noises. The shape of the MFPT curve typical for the Gaussian case vanishes much faster than for the  $H_{+} = 8, H_{-} = 0$  scenario. For a heavy tailed ( $\alpha = 0.5$ ) external noise driving (right panel of Fig. 6) the RA is not visible.

Analogously to the both previously studied barrier setups with asymmetric stable driving noises (Fig. 7) there exists an optimal  $\alpha$  for which activation processes are most efficient. Also, the RA phenomenon is inhibited at low values of  $\alpha$ , reappears for  $\alpha \approx 1$  and smears out for moderate  $\alpha$ -s before its recovery becomes effective at  $\alpha = 2$ .

By inspection of Figs. 3, 5 and 7 it can be concluded that the same kind of resonant behavior (described by a nonmonotonic shape of the MFPT curves) can be observed not only for equilibrium fluctuations but also for heavy-tailed nonequilibrium fluctuations modelled by an asymmetric noise with the stability index  $\alpha \approx 1$ . Closer analysis of the MFPT( $\alpha, \gamma$ )-surface cross-sections shows that the phenomenon disappears for very small  $\alpha$  (except of the  $H_{\pm} = \pm 8$  case), becomes induced for  $\alpha \approx 1$ , disappears for  $\alpha > 1$  and reenters again in the Gaussian limit. Note that the Gaussian cases ( $\alpha = 2$ ) have not been plotted in the figures with cross sections due to the fact that values of the MFPT for the Gaussian driving noise are significantly higher than for all other stable noises with smaller values of  $\alpha$ . Therefore Fig. 1 presents separately results of numerical analysis for  $\alpha = 2$ .

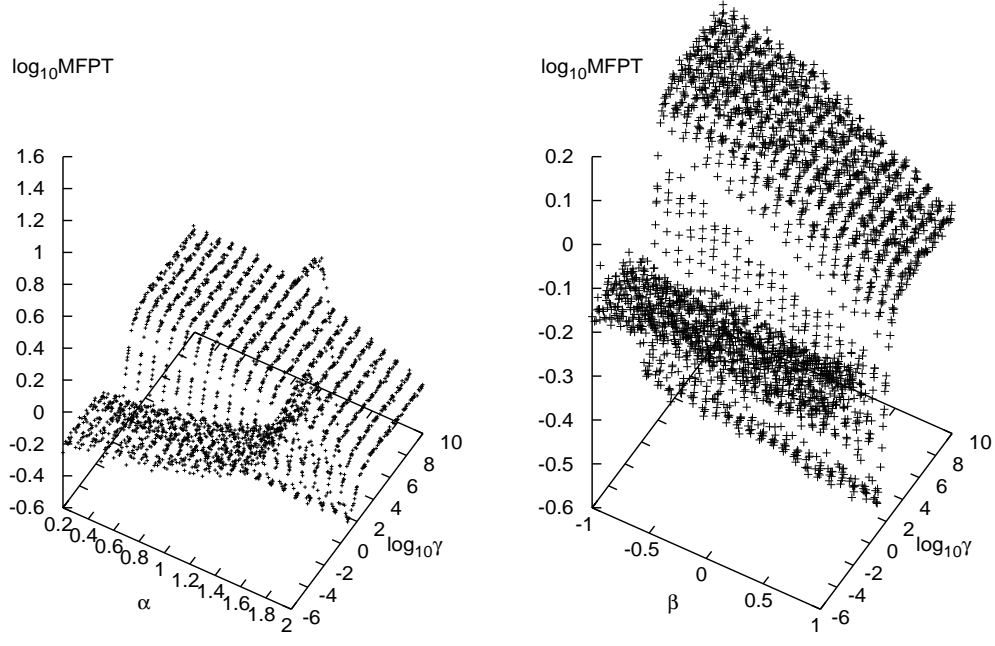


FIG. 2:  $\text{MFPT}(\alpha, \gamma)$  for  $\beta = 0$  (left panel) and  $\text{MFPT}(\beta, \gamma)$  for  $\alpha = 0.5$  (right panel) for the linear potential barrier switching between  $H_{\pm} = \pm 8$ . The results were calculated by direct integration of Eq. (1) with the time step  $dt = 10^{-4}$  and averaged over  $N = 10^3$  realizations.

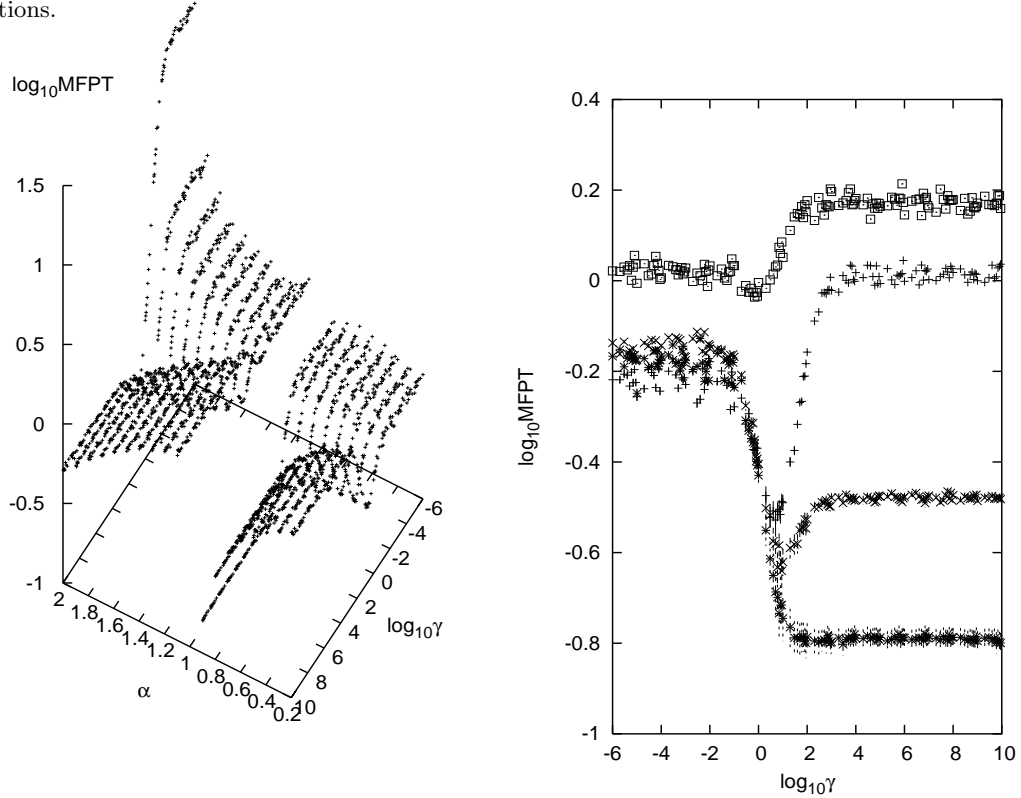


FIG. 3:  $\text{MFPT}(\alpha, \gamma)$  for  $H_{\pm} = \pm 8$  and  $\beta = 1$  (left panel) and sample cross-sections  $\text{MFPT}(\gamma)$  for various  $\alpha$ : (+)  $\alpha = 0.2$ ; ( $\times$ )  $\alpha = 0.8$ ; (\*)  $\alpha = 0.9$ ; ( $\square$ )  $\alpha = 1.1$  (right panel). The results were calculated by direct integration of Eq. (1) with the time step  $dt = 10^{-4}$  and averaged over  $N = 10^3$  realizations. Error bars represent deviation from the mean.

Examination of left panels in Figs. 2, 4 and 6 allows to see how the typical Gaussian behavior of the MFPT

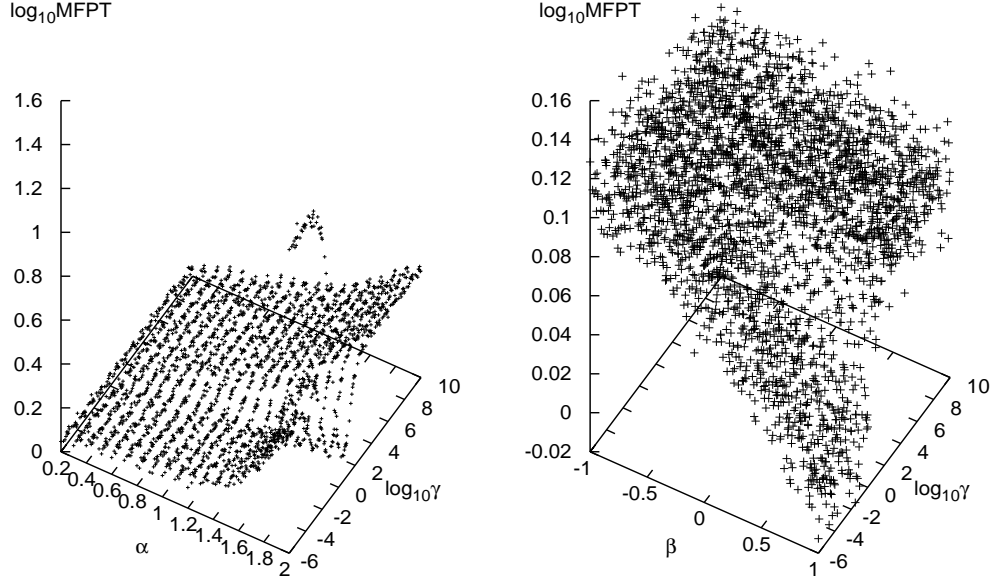


FIG. 4:  $\text{MFPT}(\alpha, \gamma)$  for  $\beta = 0$  (left panel) and  $\text{MFPT}(\beta, \gamma)$  for  $\alpha = 0.5$  (right panel) for the linear potential barrier switching between  $H_+ = 8$ ,  $H_- = 0$ . The results were calculated by direct integration of Eq. (1) with the time step  $dt = 10^{-4}$  and averaged over  $N = 10^3$  realizations.

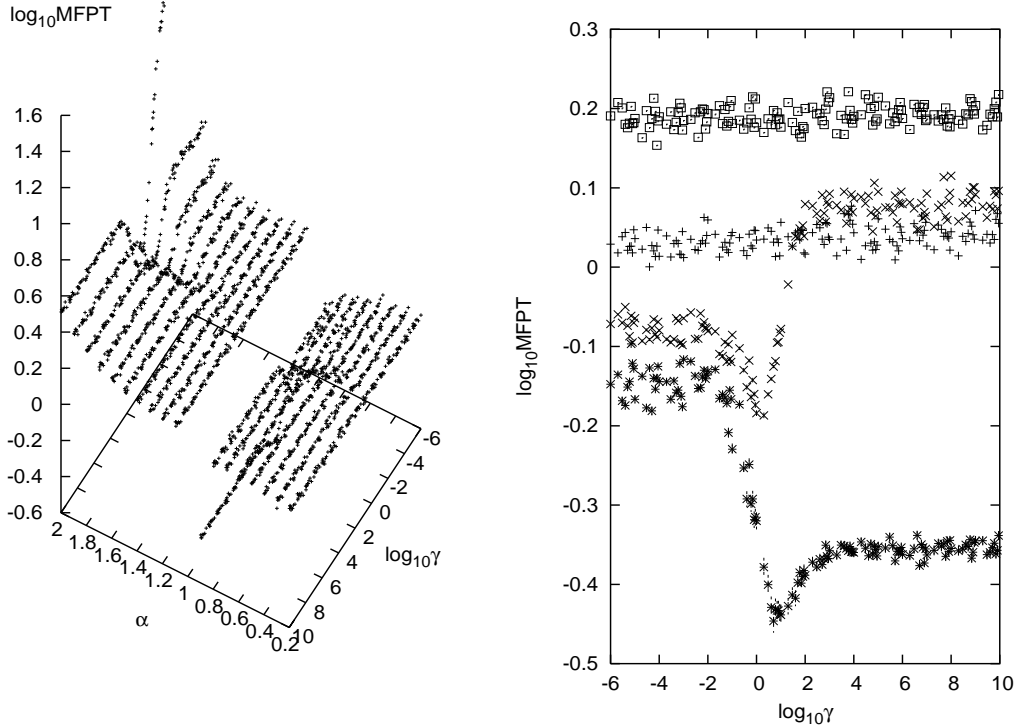


FIG. 5:  $\text{MFPT}(\alpha, \gamma)$  for  $H_+ = 8$ ,  $H_- = 0$  and  $\beta = 1$  (left panel) and sample cross-sections  $\text{MFPT}(\gamma)$  for various  $\alpha$ :  $(+)$   $\alpha = 0.2$ ;  $(\times)$   $\alpha = 0.8$ ;  $(*)$   $\alpha = 0.9$ ;  $(\square)$   $\alpha = 1.1$  (right panel). The results were calculated by direct integration of Eq. (1) with the time step  $dt = 10^{-4}$  and averaged over  $N = 10^3$  realizations. Error bars represent deviation from the mean.

curves changes with the change of the stability index  $\alpha$ . For  $H_{\pm} = \pm 8$  only changes observed are visible in the

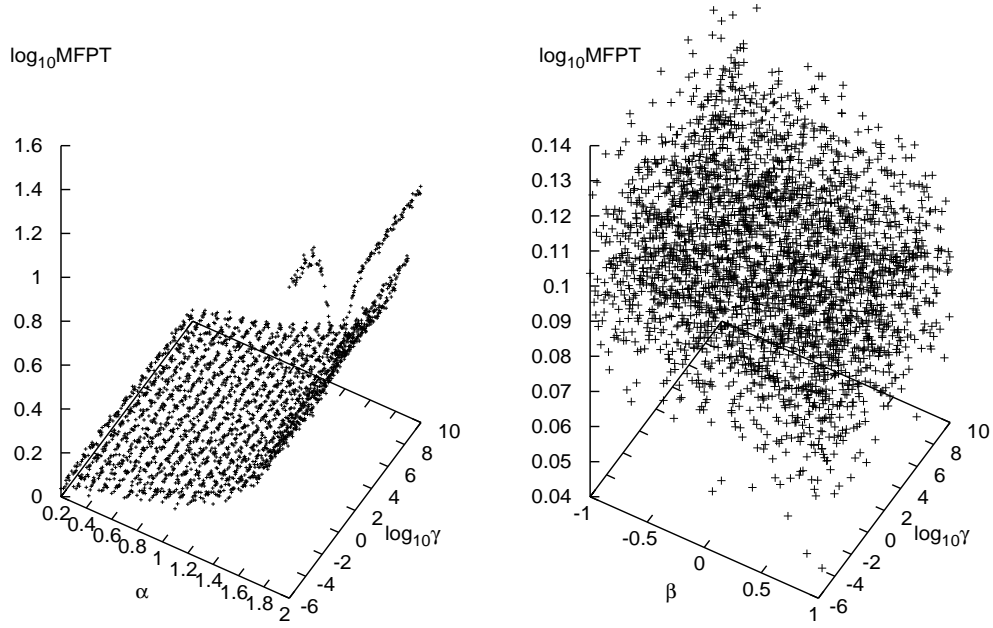


FIG. 6:  $\text{MFPT}(\alpha, \gamma)$  for  $\beta = 0$  (left panel) and  $\text{MFPT}(\beta, \gamma)$  for  $\alpha = 0.5$  (right panel) for the linear potential barrier switching between  $H_+ = 8$ ,  $H_- = 4$ . The results were calculated by direct integration of Eq. (1) with the time step  $dt = 10^{-4}$  and averaged over  $N = 10^3$  realizations.

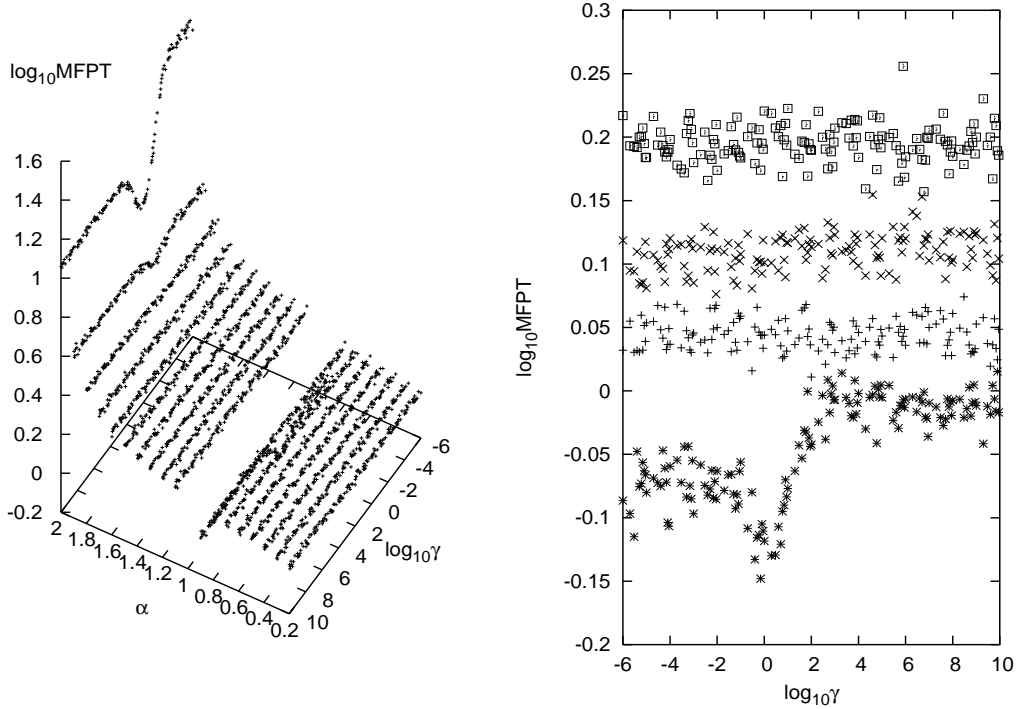


FIG. 7:  $\text{MFPT}(\alpha, \gamma)$  for  $H_+ = 8$ ,  $H_- = 4$  and  $\beta = 1$  (left panel) and sample cross-sections  $\text{MFPT}(\gamma)$  for various  $\alpha$ :  $(+)$   $\alpha = 0.2$ ;  $(\times)$   $\alpha = 0.8$ ;  $(*)$   $\alpha = 0.9$ ;  $(\square)$   $\alpha = 1.1$  (right panel). The results were calculated by direct integration of Eq. (1) with the time step  $dt = 10^{-4}$  and averaged over  $N = 10^3$  realizations. Error bars represent deviation from the mean.

asymptotic behavior of the MFPTs. For other cases under the study ( $H_+ = 8$ ,  $H_- = 0$ ;  $H_+ = 8$ ,  $H_- = 4$ ),

the typical shape of the MFPT curve disappears with decreasing  $\alpha$  and the RA phenomenon vanishes. The process is the most rapid for  $H_+ = 8$ ,  $H_- = 4$  (cf. left panel of the Fig. 6) while for  $H_+ = 8$ ,  $H_- = 0$  it slows down and becomes smoother (cf. left panel of the Fig. 4).

#### IV. SUMMARY

We have considered a thermally activated process that occurs in a system coupled to a non-Gaussian noise source introduced by a non-equilibrated thermal bath. Another external stochastic process is assumed to be responsible for dichotomous fluctuations of the potential barrier which has been modeled by the linear function with a varying slope.

The applied procedures enable to study the RA phenomena for all possible values of  $\alpha, \beta, \sigma, \mu$  mimicking statistical properties of the driving stable noises. In particular, for  $\alpha = 2$  (and any value of  $\beta$ ), the  $\alpha$ -stable noise generated by the recipe given by Eq. (11) is a Gaussian noise and numerically constructed results are in a perfect agreement with the exact results obtained by numerical integration of an appropriate backward Fokker-Planck equation [11]. In this case the RA takes place for all barrier setups under consideration. For  $\alpha = 0.5, \beta = 1$  and  $\alpha = 1, \beta = 0$  formerly studied [17] Lévy-Smirnoff and Cauchy cases were recovered. Results of numerical analysis presented in this paper agree with previously constructed solutions [17].

In the case of driving stable noises, the RA phenomenon is most resistant for the  $H_{\pm} = \pm 8$  scenario where it is visible for all noises under the study. For symmetric stable noise it is possible to observe how the Gaussian behavior of the MFPT curves changes and the RA phenomenon in the system switching between two barriers ( $H_+ = 8$ ,  $H_- = 4$ ) or barrier and no barrier ( $H_+ = 8$ ,  $H_- = 0$ ) vanishes. A novel behavior has been registered for nonsymmetric stable noises: For very small values of the stability index  $\alpha$ , the RA is not effective (except of the  $H_{\pm} = \pm 8$  case). The phenomenon reappears by increasing  $\alpha$  to  $\approx 1$ , vanishes for  $\alpha > 1$  and becomes again observable for  $\alpha = 2$  (the Gaussian case). Moreover, in the  $\alpha$  space another kind of phenomenon, allowing to choose an optimal value of  $\alpha$  for which the MFPTs are smaller than for other values of stability index  $\alpha$ , occurs. The fact that the shape of MFPT curve for very heavy-tailed, skewed distributions representing non-Gaussian noises arising from the contact with not equilibrated bath is similar to the MFPT curve in the presence of the Gaussian fluctuations arising from the contact with equilibrated thermal bath is very interesting and makes the problem of recognition of the underlying noise more complicated. This indicates that more detailed study of “resonant phenomena” in non-equilibrium situations might be required, as has been recently also argued in other studies [20] relating to the detection of the stochastic resonance in a generic double well poten-

tial under the influence of periodic signal and a colored, non-Gaussian noise.

#### V. $\alpha$ -STABLE RANDOM VARIABLES AND $\alpha$ -STABLE LÉVY MOTION PROCESSES

The  $\alpha$ -stable variables are random variables for which the sum of random variables is distributed according to the same distribution as each variable, i.e.

$$aX_1 + bX_2 \stackrel{d}{=} cX + d, \quad (3)$$

where  $\stackrel{d}{=}$  denotes equality in a distribution sense. Real constants  $c, d$  in Eq. (3) allow for rescaling and shifting of the initial probability distribution. The characteristic function of the stable distribution can be parameterized in various ways. In the usually chosen  $L_{\alpha,\beta}(\zeta; \sigma, \mu)$  [19, 21] parameterization, a characteristic function of the Lévy type variables is given by

$$\begin{aligned} \phi(k) &= \exp \left[ -\sigma^\alpha |k|^\alpha \left( 1 - i\beta \text{sign}(k) \tan \frac{\pi\alpha}{2} \right) + i\mu k \right. \\ &\quad \left. - i\beta k \sigma^\alpha \tan \frac{\pi\alpha}{2} \right], \quad \text{for } \alpha \neq 1, \\ \phi(k) &= \exp \left[ -\sigma |k| \left( 1 + i\beta \frac{2}{\pi} \text{sign}(k) \ln |k| \right) \right. \\ &\quad \left. + i\mu k \right], \quad \text{for } \alpha = 1, \end{aligned} \quad (4)$$

with  $\alpha \in (0, 2]$ ,  $\beta \in [-1, 1]$ ,  $\sigma \in (0, \infty)$ ,  $\mu \in (-\infty, \infty)$  and  $\phi(k)$  defined in the Fourier space

$$\phi(k) = \int d\zeta e^{-ik\zeta} L_{\alpha,\beta}(\zeta; \sigma, \mu). \quad (5)$$

The above parameterization (4) is continuous, in the sense that

$$\lim_{\alpha \rightarrow 1} \sigma^\alpha (|k|^\alpha \text{sign}(k) - k) \tan \frac{\pi\alpha}{2} = -\frac{2}{\pi} \sigma |k| \text{sign}(k) \ln |k| \quad (6)$$

for every  $\sigma$  and  $k$ . Analytical expressions for stable probability distributions  $L_{\alpha,\beta}(\zeta; \sigma, \mu)$  are known only in few cases: for  $\alpha = 0.5$ ,  $\beta = 1$  resulting distribution is Lévy-Smirnoff

$$\begin{aligned} L_{1/2,1}(x; \sigma, \mu) &= \left( \frac{\sigma}{2\pi} \right)^{\frac{1}{2}} (x - \mu)^{-\frac{3}{2}} \\ &\quad \times \exp \left( -\frac{\sigma}{2(x - \mu)} \right), \end{aligned} \quad (7)$$

for  $\alpha = 1$ ,  $\beta = 0$  it results in the Cauchy distribution

$$L_{1,0}(x; \sigma, \mu) = \frac{\sigma}{\pi} \frac{1}{(x - \mu)^2 + \sigma^2}, \quad (8)$$

whereas for  $\alpha = 2$  with arbitrary  $\beta$  the PDF is Gaussian. Characteristic feature of distributions  $L_{\alpha,\beta}(\zeta; \sigma, \mu)$  is existence of moments of order  $\alpha$ , i.e. the integral

$\int_{-\infty}^{\infty} L_{\alpha,\beta}(\zeta; \sigma, \mu) \zeta^\alpha d\zeta$  is finite. This statement results in the conclusion that the only stable distribution possessing the second moment is a Gaussian one; for all other values of  $\alpha$  the variance of a stable distribution diverges, and for  $\alpha \leq 1$  also the average value does not exist.

For the purpose of analysis, the corresponding Langevin equation (1) has been simulated by use of the appropriate numerical methods. Position of the particle has been obtained by direct integration of Eq. (1)

$$\begin{aligned} x(t) &= - \int_{t_0}^t [V'(x(s)) - g\eta(s)] ds + \int_{t_0}^t dL_{\alpha,\beta}(s) \\ &= - \int_{t_0}^t V'_\pm(x(s)) ds + \int_{t_0}^t dL_{\alpha,\beta}(s). \end{aligned} \quad (9)$$

In general [14, 19, 21], the  $L_{\alpha,\beta}$  measure in Eq. (9) can be approximated by

$$\begin{aligned} \int_{t_0}^t f(s) dL_{\alpha,\beta}(s) &\approx \sum_{i=0}^{N-1} f(i\Delta s) M_{\alpha,\beta}([i\Delta s, (i+1)\Delta s)) \\ &\stackrel{d}{=} \sum_{i=0}^{N-1} f(i\Delta s) \Delta s^{1/\alpha} \varsigma_i, \end{aligned} \quad (10)$$

where  $\varsigma_i$  is distributed with the PDF  $L_{\alpha,\beta}(\varsigma; \sigma = \frac{1}{\sqrt{2}}, \mu = 0)$ ,  $N\Delta s = t - t_0$  and  $M_{\alpha,\beta}([i\Delta s, (i+1)\Delta s))$  is the measure of the interval  $[i\Delta s, (i+1)\Delta s)$ .

Random variables  $\varsigma$  corresponding to the characteristic function (4) can be generated using the Janicki–Weron algorithm [19]. For  $\alpha \neq 1$  their representation is

$$\begin{aligned} \varsigma &= D_{\alpha,\beta,\sigma} \frac{\sin(\alpha(V + C_{\alpha,\beta}))}{(\cos(V))^{\frac{1}{\alpha}}} \\ &\times \left[ \frac{\cos(V - \alpha(V + C_{\alpha,\beta}))}{W} \right]^{\frac{1-\alpha}{\alpha}} + B_{\alpha,\beta,\sigma,\mu}, \end{aligned} \quad (11)$$

with constants  $B, C, D$  given by

$$B_{\alpha,\beta,\sigma,\mu} = \mu - \beta \sigma^\alpha \tan\left(\frac{\pi\alpha}{2}\right), \quad (12)$$

$$C_{\alpha,\beta} = \frac{\arctan\left(\beta \tan\left(\frac{\pi\alpha}{2}\right)\right)}{\alpha}, \quad (13)$$

$$D_{\alpha,\beta,\sigma} = \sigma \left[ \cos\left(\arctan\left(\beta \tan\left(\frac{\pi\alpha}{2}\right)\right)\right) \right]^{-\frac{1}{\alpha}}. \quad (14)$$

For  $\alpha = 1$ ,  $\varsigma$  can be obtained from the formula

$$\begin{aligned} \varsigma &= \frac{2\sigma}{\pi} \left[ \left(\frac{\pi}{2} + \beta V\right) \tan(V) - \beta \ln\left(\frac{\frac{\pi}{2}W \cos(V)}{\frac{\pi}{2} + \beta V}\right) \right] \\ &+ B_{1,\beta,\sigma,\mu}, \end{aligned} \quad (15)$$

with

$$B_{1,\beta,\sigma,\mu} = \mu + \frac{2}{\pi} \beta \sigma \ln(\sigma). \quad (16)$$

In the above equations  $V$  and  $W$  are independent random variables, such that  $V$  is uniformly distributed in the interval  $(-\frac{\pi}{2}, \frac{\pi}{2})$  and  $W$  is exponentially distributed with a unit mean [19]. Numerical integration has been performed for  $\mu = 0$  with increments of  $\Delta L_{\alpha,\beta}$  sampled from the strictly stable distributions [21], i.e. in general stable distributions generated *via* Eqs. (11)–(16) the value of  $\mu$  is shifted such that effectively  $B_{\alpha,\beta,\sigma,\mu}$  is equal to 0. Due to documented [21] numerical instability of all calculations with  $\alpha$ -stable random variables for the set  $(\alpha = 1, \beta \neq 0)$ , this case has been excluded from the analysis. Algorithms as described above have been positively tested for independence on the choice of the integration step (the evaluation of stochastic integrals with time steps  $dt = 10^{-4}$  and  $dt = 10^{-5}$  yielded the same results).

- 
- [1] Ch. R. Doering and J. C. Gadoua, *Resonant activation over a fluctuating barrier*, *Phys. Rev. Lett.* **69** (1992) 2318–2321.
  - [2] A. Fuliński, *Stochastic Resonances in Active Transport in Biological Membranes*, *Acta Phys. Pol. B* **28** (1997) 1811–1825.
  - [3] R. D. Astumian and M. Bier, *Fluctuation driven ratchets: Molecular motors*, *Phys. Rev. Lett.* **72** (1994) 1766–1169.
  - [4] E. Gudowska-Nowak, *Dynamic effects in non-adiabatic charge transfer*, *Chem. Phys.* **212** (1996) 115–123.
  - [5] S. M. Bezrukov and I. Vodyanoy, *Stochastic resonance in thermally activated reactions: Application to biological ion channels*, *Chaos* **8** (1998) 557–566.
  - [6] L. Gammaitoni, P. Hänggi, P. Jung and F. Marchesoni, *Stochastic resonance*, *Rev. Mod. Phys.* **70** (1998) 223–287.
  - [7] P. Reimann, *Brownian motors: noisy transport far from equilibrium*, *Phys. Rep.* **361** (2002) 57–265.
  - [8] M. Buguñá, J. M. Porrà, J. Masoliver and K. Lindenberg, *Properties of resonant activation phenomena*, *Phys. Rev. E* **57** (1998) 3990–4002.
  - [9] M. Marchi, F. Marchesoni, L. Gammaitoni, E. Menichella-Saetta and S. Santucci, *Resonant activation in a bistable system*, *Phys. Rev. E* **54** (1996) 3479–3487.
  - [10] J. Iwaniszewski, I. K. Kaufman, P. V. E. McClintock and A. J. McKane, *Resonances while surmounting a fluctuating barrier*, *Phys. Rev. E* **61** (2000) 1170–1175.
  - [11] B. Dybiec and E. Gudowska-Nowak, *Influence of the bar-*

- rier shape on resonant activation, *Phys. Rev. E* **66** (2002) 026123.
- [12] B. Dybiec, E. Gudowska-Nowak and P. F. Góra, *Implication of the Barrier Fluctuations on the Rate of Weakly Adiabatic Electron Transfer*, *Int. J. Mod. Phys. C* **13** (2002) 1211–1222.
- [13] B. V. Gnedenko and A. N. Kolmogorov, *Limit Distributions for sums of Independent Random Variables*, Addison-Wesley, Reading, MA (1954).
- [14] P. D. Ditlevsen, *Anomalous jumping in a double-well potential*, *Phys. Rev. E* **60** (1999) 172–179.
- [15] E. G. D. Cohen, *Statistics and dynamics*, *Physica A* **305** (2002) 19–26.
- [16] P. Garbaczewski and R. Olkiewicz, *Ornstein-Uhlenbeck-Cauchy Process*, *J. Math. Phys* **41** (2000) 6843–6860.
- [17] B. Dybiec and E. Gudowska-Nowak, *Resonant activation in the presence of non-equilibrated baths*, *Phys. Rev. E* **63** (2004) 016105.
- [18] W. Horsthemke and R. Lefever, *Noise-Induced transitions*, Springer Verlag, Berlin (1984).
- [19] R. Weron, *On the Chambers-Mallows-Stuck Method for Simulating Skewed Stable Random Variables*, *Statist. Probab. Lett.* **28** (1996) 165–171; R. Weron, *Correction to: On the Chambers-Mallows-Stuck Method for Simulating Skewed Stable Random Variables*, *Research Report HSC/96/1 Wrocław University of Technology* (1996).
- [20] C. J. Tessone, A. Plastino and H. S. Wio, *Stochastic resonance and generalized information measures*, *Physica A*, **326** (2003) 37–54.
- [21] A. Janicki and A. Weron, *Simulation and Chaotic Behavior of Stable Stochastic Processes*, Marcel Dekker, New York (1994); A. Janicki, *Numerical and Statistical Approximation of Stochastic Differential Equations with Non-Gaussian Measures*, HSC Monograph, Wrocław (1996).